Laser-assisted microscale deformation of stainless steels and ceramics

Guofei Chen
Xianfan Xu
Purdue University
School of Mechanical Engineering
West Lafayette, Indiana 47907
E-mail: xxu@ecn.purdue.edu

Chie C. Poon
Andrew C. Tam
IBM Almaden Research Center
650 Harry Road
San Jose, California 95120

Abstract. We investigate deformation of stainless steel and ceramic specimens with a precision of the order of tens of nanometers using a pulsed laser beam. Such a technique is useful, for example, in a process of removing distortions on magnetic head components to achieve a better contact between the magnetic disk head and the hard disk surface. Experiments are conducted to study the bending behavior of stainless steel and ceramics due to laser irradiation. A pulsed Nd:YLF laser beam is used to scan over the specimen to create out-of-plane deformation. The amount of deformation from each laser scan is correlated with laser and processing parameters. A theoretical model of the laser deformation process is presented based on thermo-elasticity-plasticity. The laser deformation process is explained as the result of the laser-induced nonuniform distribution of the compressive residual strain. Numerical simulations are carried out to estimate the laser-induced temperature field, the residual stress field, and the amount of deformation of the specimen. These theoretical studies help us to understand the complex phenomena involved in the pulsed-laser deformation process. [S0091-3286(98)02710-X]

Subject terms: laser forming; laser bending; pulsed laser; thermal stress; curvature modification; thermomechanics.

Paper 980101 received Mar. 16, 1998; revised manuscript received June 5, 1998; accepted for publication June 17, 1998.

1 Introduction

Today electronics production is characterized by a progressive miniaturization caused by a general trend toward higher integration and package density. Corresponding to this are the challenges to traditional manufacturing processes. In computer manufacturing, one requirement to increase the storage capacity in a hard drive is to reduce the distance between the disk surface and the disk head. For computer hard disks with capacities greater than 10 Gbytes/in.^{2}, the distance between the disk head and the disk surface is as small as 10 nm during disk operation. Thus, the flatness of both the disk and the head surfaces must be controlled with a precision better than 10 nm. Deformation of the slider occurs as a result of residual stresses caused by manufacturing processes. A technique for removing curvature distortion with precision of the order of submicroradians is required.

A pulsed-laser-based technique has been attempted for removing distortions with the required precision. This process utilizes a pulsed, diode-pumped Nd:YLF laser beam with a 10-ns pulse width focused to a small spot ($\sim$20 μm diameter) through a focusing lens system. As shown in Fig. 1, the focused laser beam (pulses) scans over the target surface, raising the temperature rapidly within the skin depth of the target ($\sim$1 to 10 μm). Heating and cooling cause compressive residual strain and plastic deformation at the laser-heated area, and thus change the curvature of the specimen permanently.

Using a laser beam for the deformation or bending purpose has been investigated for sheet metal forming.[1–4] Experimentally, it has been demonstrated that a variety of complex shapes can be formed. Possibilities of using laser bending for straightening automobile body shells and forming ship bodies were reported.[1,5] In these processes, continuous wave (cw) CO_2 or YAG lasers with powers of the order of kilowatts or higher were used. Sheet metals with thicknesses as great as 1 cm were bent more than 90 deg. The advantages of laser forming over the traditional flame-forming technique are (1) the focused heat source of the laser minimizes the heat-affected zone (HAZ) to a small area near the surface, thus material degradation is reduced, and (2) the laser-forming process can be conveniently and accurately controlled by adjusting the laser parameters, including the laser power and laser beam diameter, and the processing parameters such as the scanning speed of the laser beam.

Theoretical studies of the cw laser-bending processes have been reported. The bending mechanisms were described qualitatively in several papers.[3,6,7] Three bending mechanisms were discussed, the temperature gradient mechanism, the buckling mechanism, and the upsetting mechanism. Finite difference and finite element simulations were used to calculate the bending angle due to laser irradiation.[8] Compared with the laser-bending process, more detailed, quantitative thermo-elastic-plastic deformation analyses were conducted for similar processes such as flame bending.[9–11]

In this paper, a pulsed laser is used for bending and curvature modification with a higher accuracy than that can be achieved in the cw laser-bending operation. It is ex-

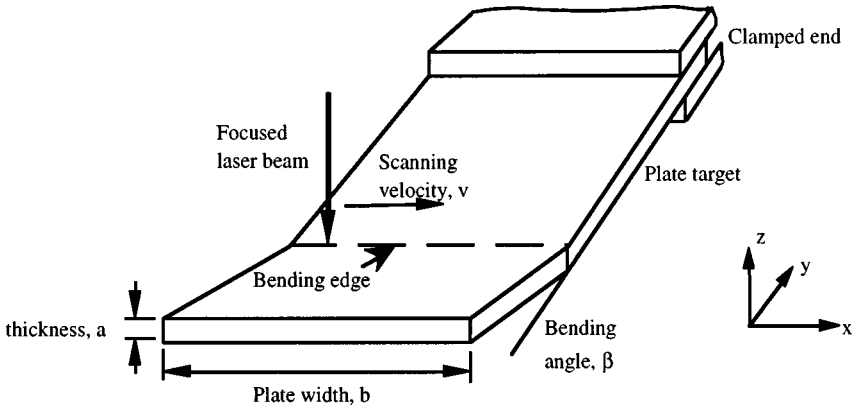

Fig. 1 Laser deformation process.

pected that the pulsed-laser-induced curvature change is influenced by many parameters, including laser energy; pulse width; spot size; overlap between laser pulses; specimen dimensions; initial stress status in the components; and the materials optical, thermal, and mechanical properties. In this paper, the theory of pulsed-laser deformation is introduced first. Experimental parametric studies of pulsed-laser bending are described next. Finally, a preliminary numerical study is used to demonstrate the theoretical explanation of the process.

2 Theory of Pulsed-Laser Deformation

The principle of pulsed-laser deformation can be explained as follows: the pulsed-laser beam raises the temperature of the irradiated area within the pulse duration of tens of nanoseconds, and a temperature gradient is established with the highest temperature at the center of the laser-heated area. Because of the short laser pulses used in this work (~10 ns), the temperature gradient in the thickness direction (*z* direction) is much higher than that obtained in cw laser operation. Even though the target used in this work is normally less than 1 mm thick, the temperature in the thickness direction is still not uniform during the heating process. During the heating period, compressive stresses arise because of thermal expansion of the heated area and the bulk constraint of the materials surrounding the heated area, as illustrated in Fig. 2. Thermal expansion of the materials causes the target to bend away from the laser beam. In high-temperature regions, plastic deformation occurs. After the laser pulse, the surface cools and the material contracts. Due to the bulk constraint, tensile stresses arise in the plastically compressed area.

The residual stress and strain at any location in the target are determined from its temperature history and the temperature-dependent stress-strain relations of the specimen. In Fig. 3, the target is considered as a linearly elastic-plastic hardening material with temperature-dependent thermal-mechanical properties. From point *A* to point *B*, the material is heated in the linear elastic region. The stress-strain relations from point *B* to point *C* (when the temperature is the maximum) and from point *C* to point *D* (the cooling period) result from the temperature-dependent thermal-mechanical properties. After the specimen cools, a compressive residual strain and a tensile residual stress are obtained. Figure 3 depicts the thermal-mechanical response of the target near the center of the laser spot, where the temperature increase is large. At other locations where the temperature rise is small, the residual stress and strain could be different from that at the center of the specimen. Because of the residual compressive strain generated near the center of the laser-irradiated area, the specimen bends in the direction toward the laser beam after cooling.

3 Experimental Study

The experimental setup for pulsed-laser deformation as well as for measuring the deformation angle is shown in Fig. 4. The laser used in this work is a pulsed diode-pumped Nd:YLF laser with a pulsed width of about 10 ns

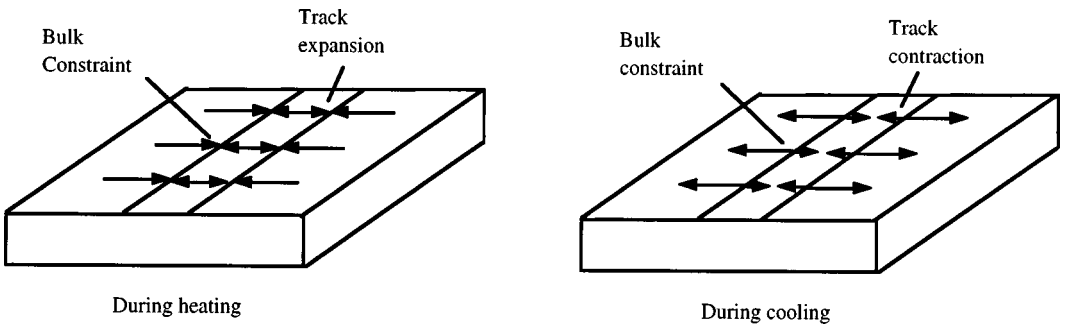

Fig. 2 Qualitative description of the laser-bending process.

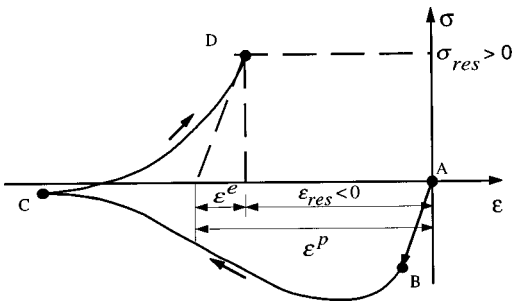

Fig. 3 Stress-strain relation at the center of laser-heated area during pulsed-laser deformation.

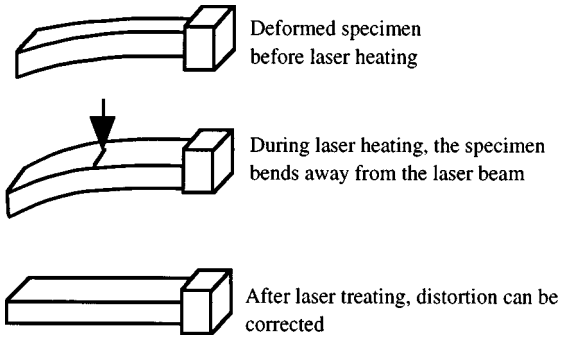

Fig. 5 Laser curvature modification process.

(FWHM) and a wavelength at 1047 nm. The pulsed-laser beam is expanded by a beam expander and focused onto the target using a focusing lens. One end of the target is clamped. The mirror and the focusing lens are mounted together on a computer-controlled motion stage, so that the laser beam size on the target surface does not change when the laser beam scans over the target surface. The computer-controlled stage scans the laser beam over the specimen surface in the x direction (the direction perpendicular to the paper), while bending is mainly achieved in the z direction. The two-axis motion stage is controlled by two closed-loop precision linear actuators, each with a velocity accuracy better than 0.2%.

To measure the out-of-plane bending angles in the z direction, a HeNe laser beam is focused at the free end of the specimen. The reflected HeNe laser beam is received by a position-sensitive detector whose position sensitivity is about 1 μm. When the distance between the sensor and the specimen is long enough, a small movement at the free end of the specimen produces a measurable displacement of the laser beam at the position sensor. This position change of the HeNe laser beam at the sensor is recorded by an oscilloscope, and is converted to the bending angle of the specimen using straightforward geometrical calculations. Using a 1.5-m distance between the sensor and the specimen, it is calculated that the sensitivity of the bending angle measurement is about 0.33 μrad. The whole experimental apparatus is set on a vibration-isolation table to avoid environmental disruption.

Stainless steel and ceramic (Al_2O_3/TiC) are used as target materials. The bending angles achieved are as small as the measurement sensitivity, $\sim$0.33 μrad. Depending on the length of the specimen, this bending angle corresponds to a movement at the free end of about 10 to 50 nm. Therefore, bending or deformation can be precisely controlled by the use of laser pulses. The thickness of the steel specimen is 0.2 mm. Before laser irradiation, the stainless steel specimen is annealed at 400°C for half an hour to relieve initial stresses caused in specimen preparation. For every laser-processing condition, it is found that the specimen bends away from the laser beam during laser heating, and toward the laser beam after laser irradiation (as shown in Fig. 5). This experimental observation agrees with the theoretical explanation of the pulsed-laser deformation process.

Bending angles are measured at various laser-processing conditions. Figure 6(a) shows the measured bending angle of stainless steel specimens obtained by a single scan of the laser beam across the specimen surface in the x direction. The laser energy per pulse is 80 μJ and the laser beam diameter at the specimen surface is about 20 μm. The scanning velocity of the laser beam is kept at a constant of 0.15 mm/s, and the frequency of the laser pulse is varied between 1 and 2000 Hz. When laser frequency increases, the distance between two adjacent laser spots decreases. The overlap between laser spots occurs when the laser frequency is higher than 8 Hz. At a pulse frequency of 200 Hz, the overlap between laser pulses is about 96%, and at a pulse frequency of 2000 Hz, the overlap between laser pulses is over 99%. Figure 6(a) shows that the obtained bending angle increases with the laser pulse frequency up

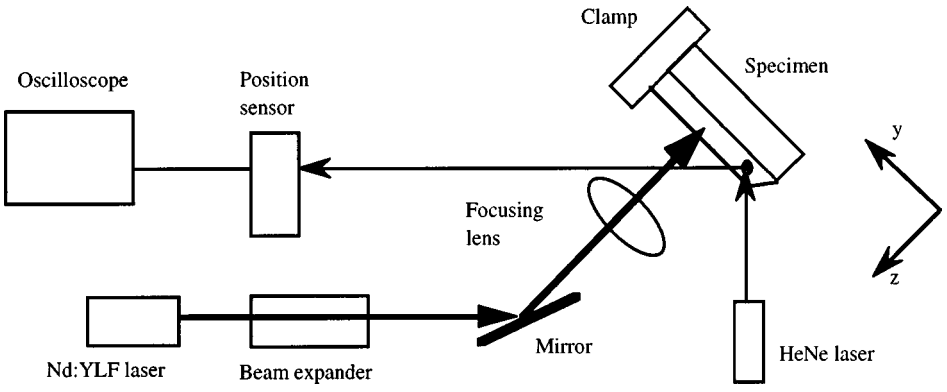

Fig. 4 Experimental setup.

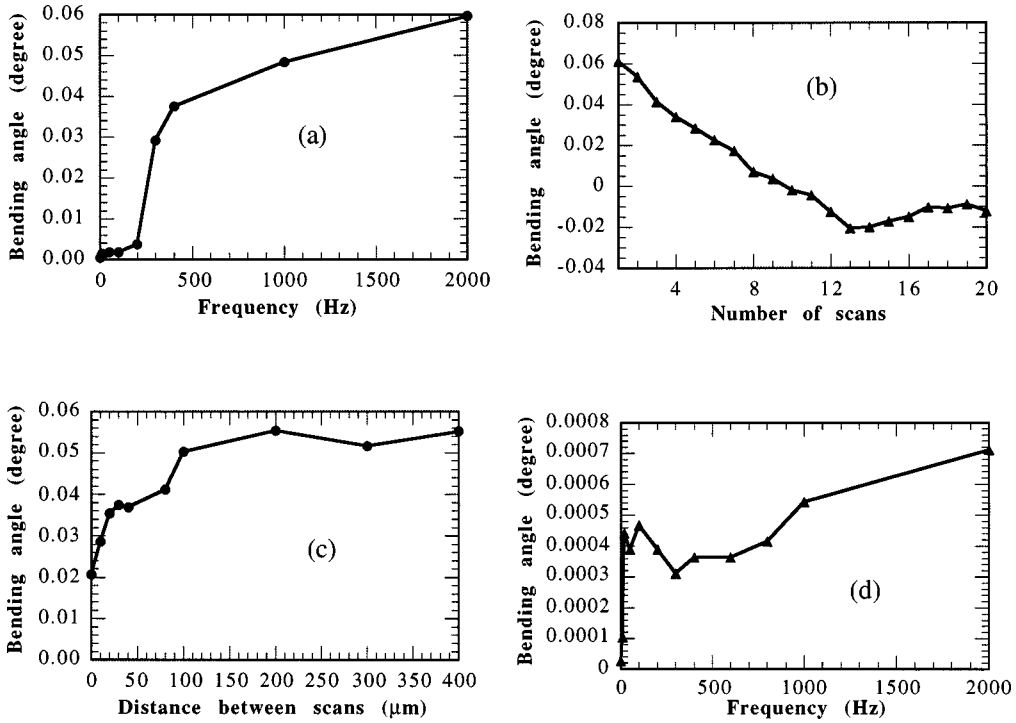

Fig. 6 Bending angle of stainless steel [(a)–(c)] and ceramic (d) as a function of (a) overlapping between laser pulses, (b) repetitive laser scans, (c) distances between laser scans, and (d) overlap between laser pulses.

to 2000 Hz. When the frequency of the laser pulse is higher than 2000 Hz, the bending angle decreases due to the decrease of laser energy per pulse. At a laser frequency of 4000 Hz, the bending angle is about 0.047 deg, and at a laser frequency of 10000 Hz, the bending angle is only 0.015 deg.

Bending with overlapping laser pulses is influenced by both the number of laser pulses and the stress produced by the laser. With more overlapping, the new pulse irradiates on the location that has been irradiated by previous laser pulses. Since the laser irradiation generates tensile residual stress (as shown in Fig. 3), it requires a higher temperature to reach the compressive yield stress when the temperature rises. The areas irradiated by previous pulses become hardened, which is known as the effect of strain hardening of laser forming.[12] Correspondingly, less additional compressive strains or bending is obtained. On the other hand, the increase of total pulses increases bending angle. These two contrary aspects determine the influence of pulse overlapping on the bending angle.

Bending angles as a function of multiple laser scans at the same location on the specimen are studied. The laser pulse energy and diameter are the same as those in the previous test. The pulse frequency is maintained at 2000 Hz. Figure 6(b) indicates that scanning over the target surface repetitively would increase bending, but the amount of additional bending achieved is less than what is obtained from a fresh surface. When the same location on the target surface is scanned more than 10 times, no bending or bending in the opposite direction could occur. These results show that the laser-induced residual stresses and strain could be saturated after a large number of laser pulses. The reason for the occurrence of saturation is the initial stress and strain hardening effects discussed previously.

If multiple laser scans are not applied to the same location on the specimen, but separated by a distance, the obtained bending angle is expected as a function of the separation distance. Variations of the bending angle with the distance between two adjacent scans are shown in Fig. 6(c). After the first scan, the second scan is located 400 μm apart, and then the third scan is 300 μm away from the second one, and so on. Figure 6(c) shows that the bending angle is almost a constant when the spacing between laser scans is greater than 100 μm. However, when the distance between laser scans is less than 100 μm, the additional bending angle achieved by the new laser scan decreases. This indicates the stress- and strain-affected zone produced with the processing condition used in this paper is about 50 μm wide. Due to the same reason as in the two experiments described previously, when the distance between two scans becomes smaller, the tensile stresses in the stress-affected zone decrease the compressive strains, therefore, bending angles created by new scans decrease.

Similar trends of the variation of the bending angle with processing parameters are obtained for ceramics as for the steel specimens. The thickness of the ceramic specimen used in this work is 0.45 mm. The result of the bending angle of the ceramic specimen as a function of pulse frequency, with a constant laser energy of 80 μJ and a beam spot of 20 μm, is shown in Fig. 6(d). The bending angle obtained for ceramics is more than one order of magnitude lower than that of the stainless steel because the ceramic specimens are thicker and have higher brittleness (lower ductility).

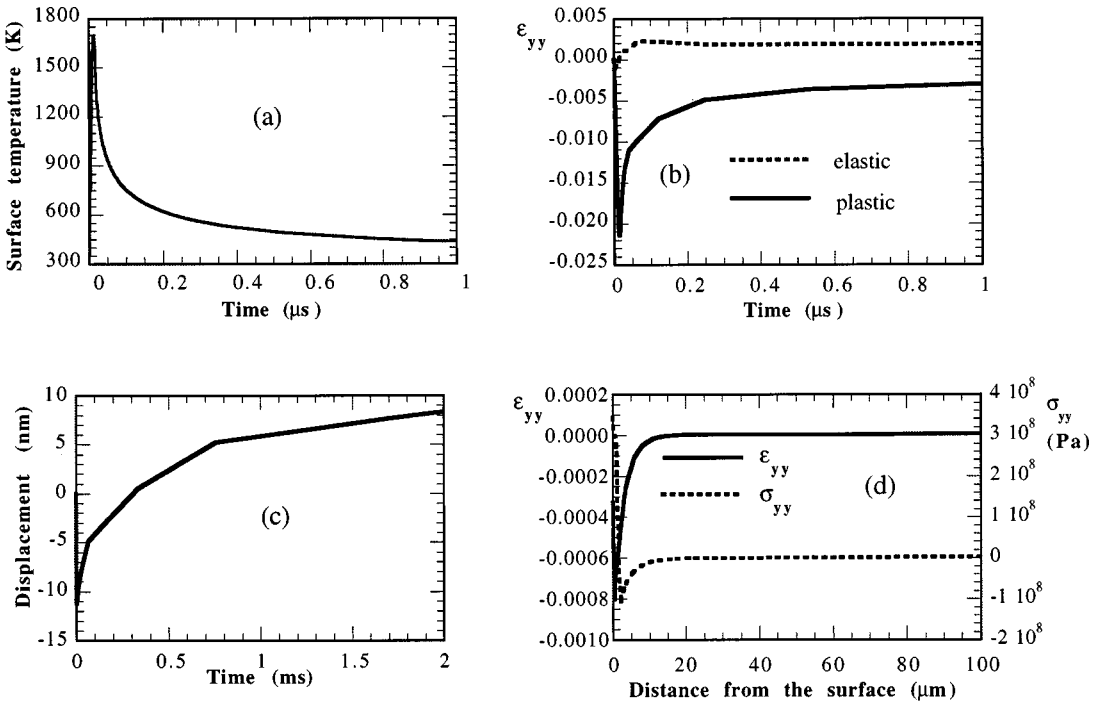

Fig. 7 Results of numerical simulation of the laser-bending process: (a) surface temperature history, (b) strain history, (c) displacement history, and (d) residual strain and stress. The laser energy density is 0.21 J/cm^2, beam width is 20 μm, and the steel specimen is 1 mm long and 100 μm thick.

4 Numerical Study

To elucidate the relation between the processing parameters and the resulting bending, numerical simulations of the laser bending process are attempted. Due to the complexities of the process, the transient temperature and stress fields in the pulsed-laser deformation process can only be obtained using numerical techniques. A preliminary numerical simulation is performed to calculate bending of a steel specimen by a line-shape laser beam, using the decoupled 2-D heat conduction equation and plane strain equations. The temperature of the target induced by laser irradiation is computed first using the 2-D transient conduction equation, treating the laser irradiation as instantaneous volumetric heat generation. The calculated transient temperature field is then used to calculate the transient stress, strain, and displacement. The mathematical descriptions of the thermal-mechanical problem include the strain-displacement relation, force equilibrium, and constitutive relations between the stress and the strain. The total strain rate is assumed to be the summation of the elastic, plastic, and thermal components. The von Mises yield criterion is used.

Only bending of stainless steel specimens is computed since the thermal and mechanical properties of ceramics are largely unknown. The steel target is modeled as a linearly elastic-plastic hardening material with temperature-dependent properties. With rather simple boundary conditions of this problem, the displacement, strain (rate), stress, and residual strain and stress are calculated. The plastic deformation is computed using the standard incremental strain rate technique. A nonlinear finite element solver (ABAQUS*) is employed for the calculation.

Figure 7 shows the computational results for a 1-mm-long, 100-μm-thick steel specimen irradiated by a laser pulse with an energy density of 0.21 J/cm^2. The laser pulse width is 10 ns and the laser beam width is 20 μm. The laser and target parameters used in the computation are different from those used in experiments. In the numerical simulation, the laser beam is treated as infinitely long in the x direction, while in experiments, a circular beam with a Gaussian intensity distribution is scanned in the x direction. The results of this numerical simulation are therefore not expected to match the experimental data. However, simulation of the scanning of the Gaussian laser beam is a much more complicated task requiring 3-D calculation, and is computational intensive. On the other hand, a much simplified, 2-D computation illustrates the fundamental physical phenomena during the pulsed-laser deformation process, and enables us to examine the theoretical descriptions of the laser-bending mechanisms.

Figure 7(a) shows the surface temperature at the center of the laser irradiated area. The temperature reaches its peak value of about 1700 K within the laser pulse duration. With the prescribed laser energy density, the maximum temperature obtained is near the melting temperature of the steel. The specimen cools to a temperature less than 450 K in less than 1 μs. After another 2 ms, the specimen cools to a temperature within 0.1 K from its initial temperature. The change of the plastic and elastic strains at the center of the

*HKS, Inc., Pawtucket, Rhode Island.

surface closely follows the temperature change as shown in Fig. 7(b). These numerical results for the transient elastic and plastic strains agree qualitatively with the theoretical description given previously, i.e., compressive plastic and elastic strains develop during the heating period; the residual plastic strain is compressive but the residual elastic strain is tensile, which agrees with what depicted in Fig. 3.

The beam deflection history shown in Fig. 7(c) also agrees with the theoretical prediction and experimental observation—bending is in the direction away from the laser beam during heating and is toward the laser beam during cooling. Notice that it takes the full cooling period, about 2 ms, to complete the bending process. Figure 7(d) shows the residual stress and strain distribution along the target surface. At the center of the laser-irradiated area when the temperature rise is the highest, compressive residual strains (the summation of elastic and plastic components) and tensile stresses are obtained after cooling, which agrees with the theoretical description. This preliminary numerical study has shown that the laser bending can be explained with the thermal-elastic-plastic theory, and it also demonstrated the possibility of using numerical simulations to investigate the pulsed-laser deformation process.

5 Conclusions

This paper demonstrated using a pulsed laser to deform metal and ceramic components with high precision. Experimental studies were conducted to find out the relations between the obtained amount of deformation and processing parameters. Laser-induced deformation was interpreted as the laser-induced thermo-elastic-plastic deformation in the target materials. A preliminary numerical study was carried out to compute the laser-induced temperature field, the residual stress and strain field, and the amount of deformation of the stainless steel specimen. Results of experimental and numerical studies showed qualitative agreement with the theoretical explanation of the pulsed-laser deformation process.

Acknowledgments

Support of this work by the Purdue Research Foundation is gratefully acknowledged. G. C. and X. X. would also like to thank Professor Klod Kokini of the School of Mechanical Engineering, Purdue University, for many valuable discussions.

References

1. K. Scully, ''Laser line heating,'' *J. Ship Prod.* **3**(4), 237–246 (1987).
2. Y. Numba, ''Laser forming of metals and alloys,'' in *Proc. Laser Advanced Materials Processing*, pp. 601–606, High Temperature Society of Japan (1987).
3. M. Geiger and F. Vollertsen, ''The mechanisms of laser forming,'' *CIRP Ann.* **42**(1), 301–304 (1993).
4. F. Vollertsen and M. Geiger, ''Systems analysis for laser forming,'' *Trans. NAMRI/SME* **23**, 33–38 (1995).
5. M. Geiger, F. Vollertsen, and G. Deinzer, ''Flexible straightening of car body shells by laser forming,'' *Sheet Metal and Stamping Symposium SAE Special Publication*, pp. 37–44, SAE, Warrendale, PA (1993).
6. M. Geiger, F. Vollertsen, and R. Kals, ''Fundamentals on the manufacturing of sheet metal microparts,'' *CIRP Ann.* **45**(1), 277–282 (1996).
7. H. Arnet and F. Vollertsen, ''Extending laser bending for the generation of convex shapes,'' *Proc. Instn. Mech. Engrs.* **209**, 433–442 (1995).
8. F. Vollertsen, M. Geiger, and W. M. Li, ''FDM- and FEM-simulation of laser forming: a comparative study,'' in *Advanced Technology of Plasticity*, Z. R. Wang and Y. He, Eds., pp. 1793–1798, International Academic Publishers, Beijing, China (1993).
9. R. E. Holt, ''Flame straightening basics,'' *Weld. Eng.* **50**, 49–52 (1965).
10. Y. Iwamura and E. F. Rybicki, ''A transient elastic-plastic thermal stress analysis of flame forming,'' *J. Eng. Indust.* 163–171 (1973).
11. A. Moshaiov and W. S. Vorus, ''The mechanics of the flame bending process: theory and applications,'' *J. Ship Res.* **31**(4), 269–281 (1987).
12. A. Sprenger, F. Vollertsen, W. M. Steen, and K. Watkins, ''Influence of strain hardening on laser bending,'' in *Proc. Laser Assisted Net Shape Engineering*, Vol. 1, pp. 361–370, Meisenbach Bamberg (1994).

Guofei Chen received his BS degree from University of Science and Technology of China in 1990 and his MS degree from Institute No. 41 of China Aerospace Corporation in 1995. He is currently a PhD student in the School of Mechanical Engineering, Purdue University. His research interests include microscale laser curvature modification of stainless steel and ceramics, laser-assisted micromachining and finite element analysis of thermal-elastic-plastic deformation.

Xianfan Xu is currently an assistant professor at the School of Mechanical Engineering of Purdue University. His research interests include mechanisms of laser-materials interaction, laser-assisted microfabrication and microprocessing, microscale energy transfer, and thermal properties of micro/nano structured materials. He is an associate member of the American Society of Mechanical Engineers, member of American Physical Society, and member of Laser Institute of America. He received his BS degree in engineering thermophysics in 1989 from the University of Science and Technology of China, and MS and PhD degrees in mechanical engineering in 1991 and 1994 from the University of California at Berkeley.

Chie C. Poon received his BE degree in engineering in 1967 from the University of Tasmania, Australia, his MS in mechanical engineering in 1970 from Syracuse University, and his PhD in mechanical engineering in 1975 from the University of California, Berkeley. He is currently a senior engineer at IBM Almaden Research Center and has worked on laser material processing, magnetic disk surface diagnostics, and particle sizing.

Andrew C. Tam is a research staff member and manager in the IBM Almaden Research Center. His research interests include optical and laser physics, spectroscopy, photothermal sensing and materials processing, and disk drive manufacturing technology, especially laser processing of materials involving ablation, laser cleaning, laser texturing and micromachining of surfaces. Dr. Tam is a fellow of the American Physical Society, fellow of the Optical Society of America, senior member of the Institute of Electronic and Electrical Engineers, and member of the Acoustic Society of America. He holds a PhD degree in physics from Columbia University, New York, 1975.